

Planar Ultra-Wideband Phase Shifter Using a Novel Type of Artificial Transmission Line

Lin Geng*, Guangming Wang, and Binfeng Zong

Abstract—An ultra-wide band 45° phase shifter based on a new planar artificial transmission line which can be used for UWB communication systems is presented. The planar artificial transmission line is composed of host line, grounded interdigital capacitors and meandered-line inductors. The phase shifter was measured to have a bandwidth about 114.7% (2.9 GHz to 10.7 GHz) for a maximum phase deviation of 2.9° , a maximum insertion loss of 1.2 dB, a minimum return loss of 13 dB and a compact size of $16.35 \text{ mm} \times 5.2 \text{ mm}$.

1. INTRODUCTION

After the U.S. Federal Communications Commission (FCC) approved the unlicensed use of ultra-wideband (UWB) (range of 3.1–10.6 GHz) for commercial purposes in 2002 [1], various UWB devices have been researched in academia and industry. As a key device, phase shifter is widely used in many microwave systems, such as intelligent antennas, phase modulators and adaptive power amplifier matching networks. So, a phase shifter with a broadband stability phase differential and low insertion loss is required for practical applications, and this can be achieved using various approaches. The Schiffman phase shifter and its improvements, which rely on edge-coupled transmission lines, are classical designs [2, 3]. However, they always take up more areas. Multilayer broadside-coupled structure is another way to build UWB phase shifters with excellent performance, but it is not the preferred option for some applications because of its uneasy fabrication [4]. A broadside-coupled microstrip-coplanar waveguide (CPW) structure is a simple and cheap manufacturing process to develop broadband phase shifters [5]. But, the existence of a defected structure on the ground is a disadvantageous factor for encapsulation. Besides, technologies, such as substrate integrated waveguide, metamaterials, and multi-section stubs technique, can also be used to develop phase shifters [6–9]. However, either a limited relative bandwidth or large size of those designed phase shifters makes them have no value in practical application for UWB systems.

Recently, the planar artificial transmission lines with a single-layer printed circuit board have attracted a lot of attention to the passive microwave components design. It has been proved that this method is a good choice to design devices with compact size and with a simple fabrication process. In this paper, a new artificial transmission line, synthesized by loading grounded interdigital structures and meandered lines on the host line, is investigated, and a compact broadband 45° planar phase shifter is realized by applying the proposed artificial transmission line. The developed phase shifter achieves low phase variation ($45.3 \pm 2.9^\circ$), low insertion loss (1.2 dB), and compact size of $16.35 \text{ mm} \times 5.2 \text{ mm}$.

Received 12 October 2015, Accepted 19 November 2015, Scheduled 24 November 2015

* Corresponding author: Lin Geng (genglin8602@163.com).

The authors are with the Air and Missile Defense College, Air Force Engineering University, Xi'an, Shaanxi 710051, China.

2. THEORY

The configuration of the proposed artificial transmission line is shown in Fig. 1(a). It is synthesized by loading the grounded interdigital structures and meander lines on the host line and printed on a substrate with height of h and dielectric constant of ϵ_r . The interdigital structures and meander lines are shorted to the ground through metallic vias. Fig. 1(b) shows the corresponding lumped equivalent circuit model. The series inductance L_0 represents the feed line. L_1 mainly represents the inner part of the host line between the interdigital capacitances, and the shunt inductance L_2 represents the grounded microstrip meandered line. C_0 is a capacitance realized by the interdigital structure. The value of the above lumped elements can be calculated by close-form expressions as in [10]:

$$L_0 \approx \frac{Z_0}{2\pi f} \tan(\beta_{eff} l) \quad (1a)$$

$$L_1 \approx \frac{Z_0}{2\pi f} \tan \left[\beta_{eff} \left(\frac{l_3}{2} - 3g_1 - 4w_1 \right) \right] \quad (1b)$$

$$L_2 \approx \frac{Z_1}{2\pi f} \tan[\beta_{eff}(w_2 + 4g_2 + 2l_2)] \quad (1c)$$

$$C_0 \approx (\epsilon_r + 1)l_1[(n - 3)A_1 + A_2] \quad (1d)$$

where

$$A_1 = 4.409 \tanh \left[0.55 \left(\frac{h}{nw_1 + (n - 1)g_1} \right)^{0.45} \right] 10^{-3} (\text{pF/mm}) \quad (2a)$$

$$A_2 = 9.92 \tanh \left[0.52 \left(\frac{h}{nw_1 + (n - 1)g_1} \right)^{0.45} \right] 10^{-3} (\text{pF/mm}) \quad (2b)$$

l and w are the length and width of the feed line, respectively. n is the finger number of the interdigital structure. l_1 , w_1 and g_1 are the coupling length between the fingers, finger width and the spacing between fingers, respectively. l_2 , w_2 , g_2 are the longitudinal length, width, and gap for the meander line, respectively. p and d are the via separation and via size, respectively. Besides, Z_0 and Z_1 are the characteristic impedance of the host line and meander line, respectively. β_{eff} is the effective phase constant in the medium. Here, it should be noted that those bends of the meander line are not taken into consideration in formula (1c).

The S -parameter of the artificial transmission line can be obtained by its overall $ABCD$ matrix as:

$$S_{11} = S_{22} = \frac{j(B - C)}{2Z_0A + j(B + C)} \quad (3a)$$

$$S_{21} = S_{12} = \frac{2Z_0}{2Z_0A + j(B + C)} \quad (3b)$$

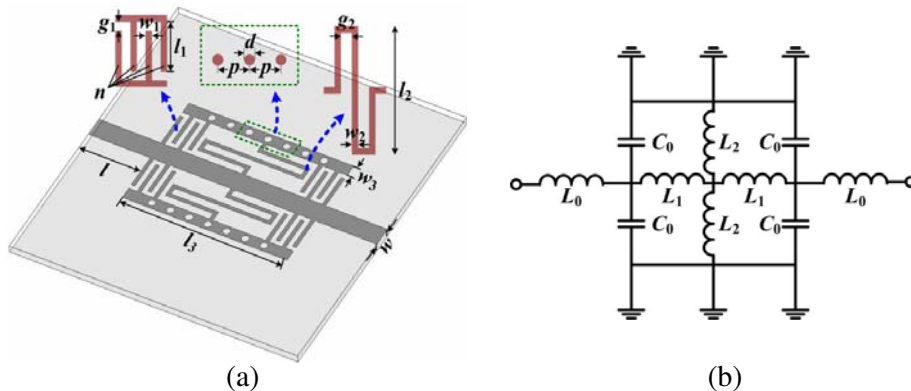


Figure 1. Proposed artificial transmission line. (a) Distributed structure. (b) Circuit model.

where

$$A = K_1 L_0 \left(\omega^2 - \frac{1}{2L_1 C_0} \right) (\omega^2 - K_2) - 1 \quad (4a)$$

$$B = j\omega K_1 L_0^2 \left(\omega^2 - \frac{L_0 + L_1}{2L_0 L_1 C_0} \right) (\omega^2 - K_2) \quad (4b)$$

$$C = \frac{K_1}{j\omega} \left(\omega^2 - \frac{1}{2L_1 C_0} \right) \left(\omega^2 - \frac{K_2 L_0}{L_0 + L_1 + L_2} \right) \quad (4c)$$

$$K_1 = \frac{8L_1(L_1 + L_2)C_0^2}{L_2} \quad (5a)$$

$$K_2 = \frac{L_0 + L_1 + L_2}{2L_0(L_1 + L_2)C_0} \quad (5b)$$

The phase shifter in this paper is composed of the proposed artificial transmission line and a normal microstrip transmission line. Here, the length and phase constant of this normal microstrip transmission line are l_m and β_{eff} , respectively. So, the differential phase shift of the output signal between them can be calculated as:

$$\Delta\Phi = \beta_{eff} l_m - \tan^{-1} \left[\frac{B + C}{2Z_0 A} \right] \quad (6)$$

To design an ultra-wide band phase shifter with good performance, the optimization objectives to minimize S_{11} , maximize S_{21} , and minimize differential phase shift of the output signal between the proposed artificial transmission line and the normal one should be built. According to [11], the following optimization objectives are used:

$$\text{Min } F_1 = \max_{f \in X} \{S_{11}(f)\} \quad (7a)$$

$$\text{Max } F_2 = \min_{f \in X} \{S_{21}(f)\} \quad (7b)$$

$$\text{Max } F_3 = \frac{1}{|X|} \sum_{f \in X} S_{21}(f) \quad (7c)$$

$$\text{Min } F_4 = \max_{f \in X} \{\Delta\Phi - \Delta\varphi\} \quad (7d)$$

$$\text{Min } F_5 = \frac{1}{|X|} \sum_{f \in X} \{\Delta\Phi - \Delta\varphi\} \quad (7e)$$

where X is a set of sampled frequencies in the design band. In these optimization objectives. Eq. (7a) is for minimizing the maximum S_{11} in the designed band. Eqs. (7b) and (7c) are for maximizing the minimum and average S_{21} , respectively. Eq. (7d) is for minimizing the maximum difference between the differential phase shift and the designed value, and Eq. (7e) is for minimizing the average difference between the differential phase shift and the designed value.

The optimization procedure is finished using the particle swarm algorithm and the HFSS in order to obtain the specific dimension values of the proposed artificial transmission line. The mathematics method is used to calculate the initial dimension values of the phase shifter while the final ones are obtained using the optimization capability of the software HFSS.

3. DESIGN AND RESULTS

For demonstrating the effectiveness of the design method, a 45° phase shifter for UWB was designed and fabricated using a substrate with a dielectric constant of 2.65 and thickness of 0.3 mm. The targets in this paper are set as $F_1 \leq 10$ dB, $F_2 \geq 1$ dB, $F_4 \leq 5^\circ$, and X ranges from 3.1 GHz to 10.6 GHz. After the optimization, the dimensions can be obtained as $l = 4.65$ mm, $w = 0.8$ mm, $l_1 = 1.49$ mm, $w_1 = 0.15$ mm, $g_1 = 0.2$ mm, $l_2 = 4.25$ mm, $w_2 = 0.15$ mm, $g_2 = 0.31$ mm, $l_3 = 7.05$ mm, $w_3 = 0.5$ mm, $d = 0.3$ mm, $p = 0.8$ mm, $n = 4$. The length of the reference line is 23.2 mm. The occupied size of the

fabricated device is $16.35 \text{ mm} \times 5.2 \text{ mm}$ (excluding the reference line). Fig. 2 shows a photograph of the fabricated device. The performance of the designed device was measured using a vector network analyzer.

Figure 3 shows the comparison between the simulated and measured S -parameters of the developed device. From the measured result we can see that the fabricated UWB phase shifter has a passband from 2.6 GHz to 11.4 GHz with a fractional bandwidth of 125.7% assuming the 10 dB return loss as a reference. The insertion loss of the proposed phase shifter is less than 0.65 dB in the simulation and less than 1.2 dB in the measurement across most part of the passband. The discrepancy between the simulation and measurement mainly comes from the fabrication error and loss of connectors. Fig. 4 shows the phase shift between the proposed artificial transmission line and the reference line (phase S_{21} -phase S_{43}). As shown in the measured result, a differential phase shift of $45^\circ \pm 5^\circ$ is achieved from 2.7 GHz to 10.9 GHz, and the bandwidth of the designed circuit is 120.6%. At the operating band of UWB (2.9–10.7 GHz), the proposed phase shifter has a maximum phase deviation of 2.9° , maximum insertion loss of 1.2 dB, and minimum of return loss of 13 dB.

Table 1 compares the frequency range, phase differential, number of layer and effective area of the

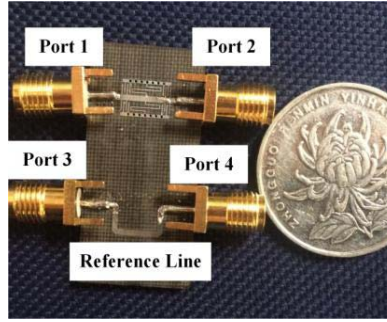


Figure 2. Photograph of the developed 45° phase shifter.

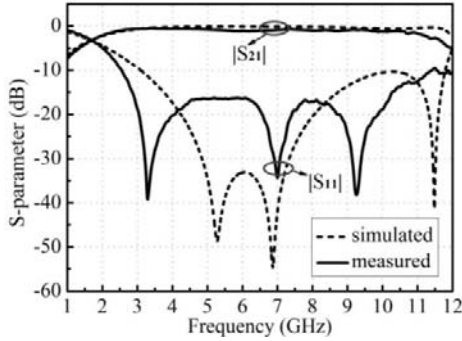


Figure 3. S -parameters of the designed phase shifter.

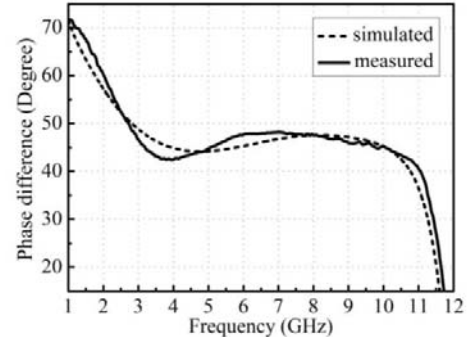


Figure 4. Phase performance of the designed phase shifter.

Table 1. Comparison of various 45° phase shifters.

	Frequency range	Phase differential	Layer	The effective area
This Work	2.9–10.7 GHz	$45.3 \pm 2.9^\circ$	1	$16.35 \times 5.2 \text{ mm}^2$
[4]	3.3–10.6 GHz	$45 \pm 2.3^\circ$	3	$25 \times 7.3 \text{ mm}^2$
[8]	2–6 GHz	$47.8 \pm 3.2^\circ$	1	$17.78 \times 10.8 \text{ mm}^2$
[9]	3.1–10.6 GHz	$45.8 \pm 4.5^\circ$	1	200 mm^2

proposed 45° phase shifter (excluding the reference line) with the those of the references. It can be found that the phase shifter in this paper is better than the referenced ones when taking properties into consideration comprehensively.

4. CONCLUSION

A new method in the design of a broadband phase shifter with a constant differential phase has been presented. The device utilizes an artificial transmission line, which enables an easy fabrication using printed circuit board's technology. A 45° phase shifter, which occupies a compact size of $16.35\text{ mm} \times 5.2\text{ mm}$, was designed using the proposed method for UWB system. The simulated and measured results of the phase shifters have shown good performances in the UWB frequency range.

ACKNOWLEDGMENT

This work was supported by the National Natural Science Foundation of China under Grant 61501501.

REFERENCES

1. "Revision of part 15 of the commission's rules regarding ultra-wideband transmission systems," First Note and Order Federal Communications Commission, ET-Docket 98-153, 2002.
2. Quirarte, J. L. R. and J. P. Starski, "Synthesis of Schiffman phase shifters," *IEEE Trans. Microw. Theory Tech.*, Vol. 39, No. 11, 1885–1889, Nov. 1991.
3. Guo, Y. X., Z. Y. Zhang, and L. C. Ong, "Improved wideband Schiffman phase shifter," *IEEE Trans. Microw. Theory Tech.*, Vol. 54, No. 3, 1196–1200, Mar. 2006.
4. Abbosh, A., "Ultra-wideband phase shifters," *IEEE Trans. Microw. Theory Tech.*, Vol. 55, No. 9, 1935–1941, Sep. 2007.
5. Abbosh, A., "Broadband fixed phase shifters," *IEEE Microw. Wireless Compon. Lett.*, Vol. 21, No. 1, 22–24, Jan. 2011.
6. Sellal, K., L. Talbi, T. A. Denidni, and J. Lebel, "Design and implementation of a substrate integrated waveguide phase shifter," *IET Microw. Antennas Propag.*, Vol. 2, No. 2, 194–199, 2008.
7. He, P., J. Gao, C. Marinis, P. Parimi, C. Vittoria, and V. Harris, "A microstrip tunable negative refractive index metamaterial and phase shifter," *Appl. Phys. Lett.*, Vol. 93, No. 19, 193505-1–193505-3, 2008.
8. Zheng, S. Y., S. H. Yeung, W. S. Chan, K. F. Man, and S. H. Leung, "Improved broadband dumb-bell-shaped phase shifter using multi-section stubs," *Electron. Lett.*, Vol. 44, No. 7, 478–480, Mar. 2008.
9. Tang, X. and K. Mouthaan, "Design of a UWB phase shifter using shunt $\lambda/4$ stubs," *IEEE MTT-S Int. Microw. Symp. Dig.*, 1021–1024, Jun. 2009.
10. Caloz, C. and T. Itoh, *Electromagnetic Metamaterials: Transmission Line Theory and Microwave Applications*, Wiley-IEEE Press, New York, 2005.
11. Yeung, S. H., Q. Xue, and K. F. Man, "Broadband 90° differential phase shifter constructed using a pair of multisection radial line stubs," *IEEE Trans. Microw. Theory Tech.*, Vol. 60, No. 9, 2760–2776, Sep. 2012.